DOI: 10.1002/JLB.MR0318-123R

JLB JOURNAL OF LEUKOCYTE BIOLOGY

REVIEW

Death, TIR, and RHIM: Self-assembling domains involved in innate immunity and cell-death signaling

Jeffrey D. Nanson[1] | **Bostjan Kobe**[1] | **Thomas Ve**[1,2]

[1]School of Chemistry and Molecular Biosciences, Institute for Molecular Bioscience and Australian Infectious Diseases Research Centre, University of Queensland, Brisbane, Queensland 4072, Australia

[2]Institute for Glycomics, Griffith University, Southport, Queensland 4222, Australia

Correspondence
Thomas Ve, Institute for Glycomics, Griffith University, Bld 26, Parklands Dr, Southport QLD 4222, Australia.
Email: t.ve@griffith.edu.au

Abstract

The innate immune system consists of pattern recognition receptors (PRRs) that detect pathogen- and endogenous danger-associated molecular patterns (PAMPs and DAMPs), initiating signaling pathways that lead to the induction of cytokine expression, processing of pro-inflammatory cytokines, and induction of cell-death responses. An emerging concept in these pathways and associated processes is signaling by cooperative assembly formation (SCAF), which involves formation of higher order oligomeric complexes, and enables rapid and strongly amplified signaling responses to minute amounts of stimulus. Many of these signalosomes assemble through homotypic interactions of members of the death-fold (DF) superfamily, Toll/IL-1 receptor (TIR) domains, or the RIP homotypic interaction motifs (RHIM). We review the current understanding of the structure and function of these domains and their molecular interactions with a particular focus on higher order assemblies.

KEYWORDS

higher-order assembly signaling, inflammasome, NOD (nucleotide binding and oligomerization domain) and leucine rich repeat containing receptor (NLR), necrosome, signaling by cooperative assembly formation (SCAF), Toll-like receptor

1 | INTRODUCTION

The innate immune system detects and protects against microorganisms and cellular damage, and it consists of 'pattern recognition receptors' (PRRs) that recognize evolutionarily conserved 'pathogen-associated molecular patterns' (PAMPs) and endogenous 'danger-associated molecular patterns' (DAMPs) released by dying or damaged cells. Activation of these receptors initiates signaling pathways to induce upregulation of cytokine expression, processing of pro-inflammatory cytokines, and programmed cell-death responses. These responses control a pathogenic infection, initiate tissue repair, and stimulate the adaptive immune system.

Structural studies have provided fundamental biological insight into how these pathways are activated and an emerging theme corresponds to 'signaling by cooperative assembly formation' (SCAF), which involves assembly of higher order complexes—signalosomes or 'supramolecular organizing centers' (SMOCs).[1–7] In the resting state, the PRRs are often auto-inhibited through intramolecular interactions, but conformational changes induced by PAMP/DAMP binding result in receptor oligomerization, which nucleates recruitment and oligomerization of cytosolic adaptor proteins, in turn nucleating recruitment and oligomerization of effector enzymes that are subsequently activated through proximity-induced mechanisms. SCAF enables PRRs

Abbrevations: Act1, NF-κB activator 1; AIM2, absent in melanoma 2; ALRs, AIM2-like receptors; APAF, apoptotic protease activating factor-1; ASC, apoptosis-associated speck-like protein containing a caspase recruitment domain; BCAP, B-cell adaptor for PI3K; BCL-10, B cell lymphoma 10; CARD, caspase recruitment domain; CBM, CARD-CC/BCL-10/MALT1-like paracaspase complex; CC, coiled coil; cFLIP, cellular FLICE-like inhibitory protein; CLR, C-type lectin domain receptor; DAI, DNA-dependent activator of IFN regulatory factor; DAMP, danger-associated molecular pattern; DD, death domain; DED, death effector domain; DEDD, death effector domain-containing protein; DF, death fold; DISC, death signaling complex; DR, death receptor; FADD, Fas-associating death domain-containing protein; FAS, first apoptotic signal receptor; IG, immunoglobulin domain; IL-17R, Interleukin-17 receptor; IL-1R, Interleukin-1 receptor; IRAK, IL-1R associated kinase; IRF, IFN regulatory factor; MAGUK, membrane-associated guanylate kinase; MAL, MyD88 adaptor-like protein; MALT1, mucosa-associated lymphoid tissue lymphoma translocation protein 1; MAVS, mitochondrial antiviral-signaling protein; MDA5, melanoma differentiation associated gene 5; MLKL, mixed lineage kinase domain-like protein; MyD88, myeloid differentiation primary response gene 88; NAD, nicotinamide adenine dinucleotide; NAIP, NLR family apoptosis inhibitory protein; NF-κB, nuclear factor kappa-light-chain-enhancer of activated B cells; NLR, NOD (nucleotide binding and oligomerization domain) and leucine rich repeat containing receptor; PAMP, pathogen associated molecular pattern; PEA-15, phosphoprotein enriched in astrocytes 15; PIDD, p53-induced protein with a DD; PRR, pattern recognition receptor; PYD, pyrin domain; PYHIN, pyrin and HIN [hematopoietic interferon-inducible nuclear localization 200] amino acid repeat domain containing family; RAIDD, RIP-associated ICH-1 homologous protein with a death domain; RHIM, RIP homotypic interaction motif; RIP, receptor-interacting protein kinase; RLR, RIG-I [retinoic acid-inducible gene 1]-like receptor; SARM, sterile-α and TIR motif containing protein; SCAF, signaling by cooperative assembly formation; SEFIR, similar expression to fibroblast growth factor genes and IL-17R domain; TLR, Toll-like receptor; TNFR, tumor necrosis factor receptor; TIR, Toll/IL-1 receptor domain; TRADD, tumor necrosis factor receptor type 1-associated protein with death domain; TRAF2, TNFR-associated factor 2; TRAM, TRIF-related adaptor molecule; TRIF, TIR domain-containing adaptor protein inducing IFN; vFLIP, viral FLICE-like inhibitory protein

Received: 11 August 2018 | Revised: 31 October 2018 | Accepted: 1 November 2018

to respond rapidly to a low-level stimulus and although it is not an exclusive mechanism to innate immunity and cell-death pathways, it is ideally suited to signaling in these pathways.

SCAF and assembly of higher order complexes have been observed in 'Toll-like receptor' (TLR)[5] and 'RIG-I (retinoic acid-inducible gene 1)-like receptor' (RLR) signaling,[8–10] in inflammasome formation initiated by 'NOD (nucleotide binding and oligomerization domain) and leucine rich repeat containing receptors' (NLRs), and 'pyrin and HIN (hematopoietic interferon-inducible nuclear localization 200) amino acid repeat domain containing family' (PYHIN) receptors,[11–13] in 'receptor-interacting protein kinase' (RIP) −1 and −3 necrosome assembly stimulated by members of the 'tumor necrosis factor' (TNF) and TLR superfamilies,[14–18] and in the assembly of 'CARD-CC/BCL-10/MALT1-like paracaspase' (CBM) complexes,[19,20] which are involved in signaling by some 'C-type lectin domain receptors' (CLRs), B- and T-cell receptors in lymphocytes, and the G protein-coupled receptor angiotensin II, and in keratinocyte immunity.[21–25] In addition, SCAF has also been proposed to play an important role in effector-triggered immunity in plants.[26,27]

These signalosomes largely form through homotypic interactions of (i) members of the 'death fold' (DF) domain superfamily, (ii) 'Toll/IL-1 receptor' (TIR) domains, or (iii) 'RIP homotypic interaction motifs' (RHIMs) (Fig. 1). Here, we review the function and structure of these domains, and the molecular interactions mediated by them.

2 | DEATH-FOLD DOMAIN SUPERFAMILY

The DF superfamily is composed of 4 subfamilies, the 'death domain' (DD), the 'death effector domain' (DED), the 'caspase recruitment domain' (CARD), and the 'pyrin domain' (PYD), which are all known to form homotypic interactions leading to the formation of oligomeric signaling assemblies such as inflammasomes and the Myddosome (Fig. 2). These domains are found in many multicellular organisms including mammals, *Drosophila*, zebrafish and *C. elegans*. DED, CARD, and PYD containing proteins are also found in some viral pathogens, where they are involved in host defense system evasion (reviewed in [28]).

Members of the DF superfamily share a common α-helix bundle (usually 6 helices, H1–H6), with helices arranged anti-parallel in a Greek key type topology surrounding a hydrophobic core (Fig. 3). The arrangement of these helices results in 6 protein binding surfaces, which mediate cooperative interactions with 3 types of interfaces (type I, II, and III). These interfaces facilitate the cooperative assembly of large, oligomeric signaling complexes, and the recruitment of effector enzymes, such as caspases and kinases, which undergo concentration-dependent proximity-induced auto-activation following assembly. Proteins rarely contain the DF domain in isolation, typically this domain is found in combination with other protein–protein interaction domains or effector domains conferring enzymatic activity.

Although all members of the DF superfamily share the same overall fold, the individual subfamilies exhibit distinct structural and sequence differences that confer a degree of specificity. Members of each subfamily interact with a specific array of binding partners. Typically, these are homotypic interactions such as that of 'apoptosis-associated speck-like protein containing a caspase recruitment domain' (ASC) CARD recruiting procaspase-1 CARD, and the DD of the TLR adaptor protein 'myeloid differentiation primary response gene 88' (MyD88) interacting with the DDs of the 'IL-1R associated kinase' (IRAK) -2 and -4. However, the CARD of 'apoptosis repressor with a CARD protein' (ARC) has been reported to interact with the DDs of the 'Fas-associating death domain-containing protein' (FADD) *in vitro*,[29] and the recruitment of procaspase-8 to inflammasomes via interaction between the ASC PYD and the procaspase tandem DED suggests heterotypic interactions also play a role in the formation of signaling complexes.[30]

2.1 | The DD subfamily

The DD serves as a homotypic protein–protein interaction domain in numerous intracellular signaling proteins involved in innate immunity and cell-death pathways (Fig. 1). Members of the death receptor subfamily of the 'tumor necrosis factor receptor' (TNFR) superfamily mediate cell-death pathways following ligand-induced oligomerization of extracellular receptor domains and subsequent recruitment of DD containing proteins through their own intracellular DDs. The death receptors, 'first apoptotic signal receptor' (Fas), 'death receptor 4' (DR4), and 'death receptor 5' (DR5) interact via a homotypic interaction with the C-terminal DD of FADD. FADD also contains an N-terminal DED and homotypically interacts with the 'tandem DEDs' (tDEDs) of procaspase-8 or -10 to form the 'death signaling complex' (DISC). Assembly of the complex activates the initiator caspases that in turn activate effector caspases, such as caspase-3 and -7, leading to apoptosis.[31–35]

Two other death receptors, TNFR1 and 'death receptor 3' (DR3), recruit the adaptor protein 'TNF receptor type 1-associated protein with death domain' (TRADD) via the N-terminal DD of TRADD. Recruitment of TRADD can facilitate either pro-cell survival and 'nuclear factor kappa-light-chain-enhancer of activated B cells' (NF-κB) activation through the DD:DD recruitment of RIP1 and 'TNFR associated factor 2' (TRAF2) termed complex I, or when RIP1 is not ubiquitylated, initiation of apoptosis via DD:DD mediated recruitment of FADD and subsequently procaspase-8, termed complex II.[36–39]

Outside of the TNFR superfamily, the DD-containing proteins, 'p53-induced protein with a DD' (PIDD) and 'RIP-associated ICH-1 homologous protein with a death domain' (RAIDD), form an assembly termed the PIDDosome via homotypic interactions between the DDs of PIDD and RAIDD, and between the N-terminal CARDs of RAIDD and procaspase-2. Similar to TRADD signaling, isoforms of PIDD have been reported to recruit RIP1, leading to NF-κB activation and cell survival.[40,41]

In addition to a C-terminal TIR domain, the TLR adaptor protein MyD88 possesses an N-terminal DD, which facilitates the assembly of an oligomeric assembly complex, termed the Myddosome, through DD:DD interactions with IRAKs, which contain an N-terminal DD and a carboxy-terminal Ser/Thr kinase or pseudokinase domain (Fig. 2). The 'MyD88 adaptor-like protein' (MAL) TIR domain nucleates the formation of MyD88 assemblies,[5] suggesting that oligomerization of the MyD88 TIR domain serves to cluster the MyD88 DDs, followed by recruitment and proximity based auto- and cross-phosphorylation

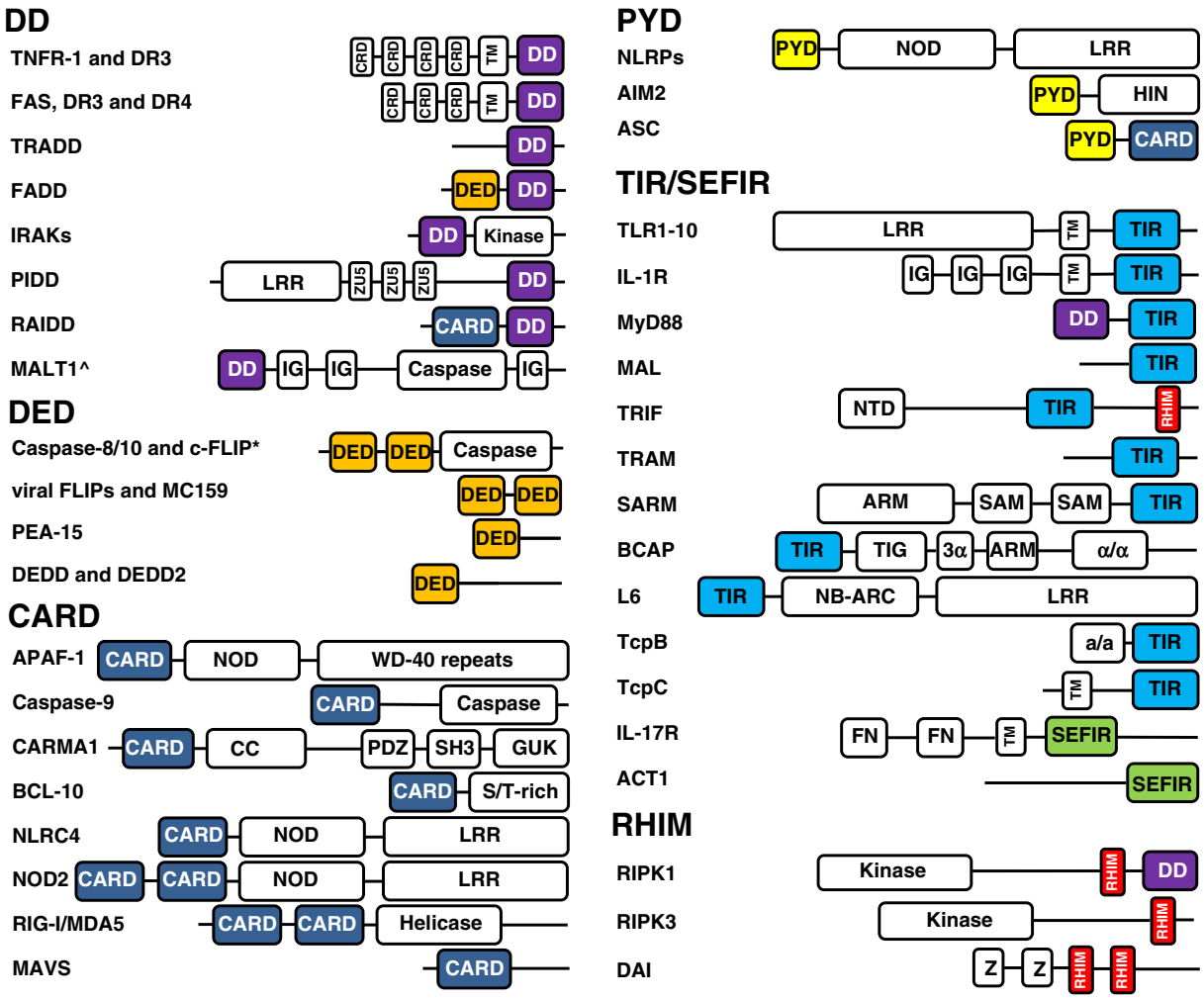

FIGURE 1 **Domain organization of selective proteins containing DF, TIR, SEFIR, and RHIM domains.** ^MALT has a paracaspase domain. *cFLIP has a pseudo-caspase domain. CRD, cysteine rich domain; TM, transmembrane; LRR, leucine rich repeat; ZU5, named after the mouse tight junction protein ZO-1 and the *C. elegans* uncoordinated protein 5; IG, immunoglobulin; NOD, nucleotide-binding oligomerization domain; WD-40, short ~40 amino acid motifs, often terminating in a Trp-Asp (W-D) dipeptide; CC, coiled coil domain; PDZ, acronym derived from the names of the first proteins in which the domain was observed in: post-synaptic density protein 95, *Drosophila* disc large tumor suppressor and zona occludens 1; SH3, SRC homology 3 domain; GUK, guanylate kinase; HIN, hematopoietic IFN-inducible nuclear antigens with a 200-amino-acid repeat; NTD, N-terminal domain; ARM, armadillo repeat motif domain; SAM, sterile alpha motif domain; TIG, Ig-like domain; 3α, 3-α-helix structural unit; α/α, helical domain; NB-ARC, nucleotide-binding domain shared by APAF-1, certain *R* gene products and CED-4; FN, fibronectin; Z, Z-DNA binding domain

of IRAKs. IRAKs in turn phosphorylate TRAF6, leading to the activation of transcription factors such as NF-κB and 'activator protein 1' (AP-1).[42–44] The structures of the DDs in the Fas/FADD DISC, PIDD/RAIDD PIDDosome, and MyD88/IRAK2/IRAK4 Myddosome complexes reveal three shared asymmetric interfaces (type I, II, and III; Fig. 3), despite the apparent differences in assembly stoichiometry and morphology.[41,42,45]

2.2 | The DED subfamily

The DED sub-family includes FADD, 'phosphoprotein enriched in astrocytes 15' (PEA-15), 'death effector domain-containing protein' (DEDD), and DEDD2, which all contain a single N-terminal DED, as well as procaspase-8 and -10, the 'cellular FLICE-like inhibitory proteins' (cFLIPs), and MC159 (viral FLIP from the Molluscum contagiosum virus), which possess tDEDs (Fig. 1). While FADD is known to interact with the tDEDs of procaspase-8 or -10 to form the DISC, the roles of PEA-15, DEDD, and DEDD2 are unknown. PEA-15 appears to have no catalytic function, acting as a modulator through protein–protein interactions. In particular, PEA-15 appears to inhibit apoptosis by binding to FADD through homotypic DD interactions and preventing the recruitment and activation of procaspases.[10–12,24] However, PEA-15 is also implicated in 'mitogen-activated protein kinase' (MAPK) signaling through a non-DD interaction with 'extracellular signal-regulated kinase' (ERK). DEDD and DEDD2 translocate to the cell nucleus and induce limited apoptotic signaling; however, when nuclear localization is prevented, DEDD and DEDD2 bind to procaspase-8 or -10 in a DED-dependent manner and induce apoptosis. The significance of this signaling *in vivo* remains unknown.[46]

The structures of the DEDs of FADD,[47] PEA-15,[48] procaspase-8,[49,50] and MC159[51] reveal that DEDs display the 6-helical bundle fold representative of the DF superfamily (Fig. 3). In comparison to

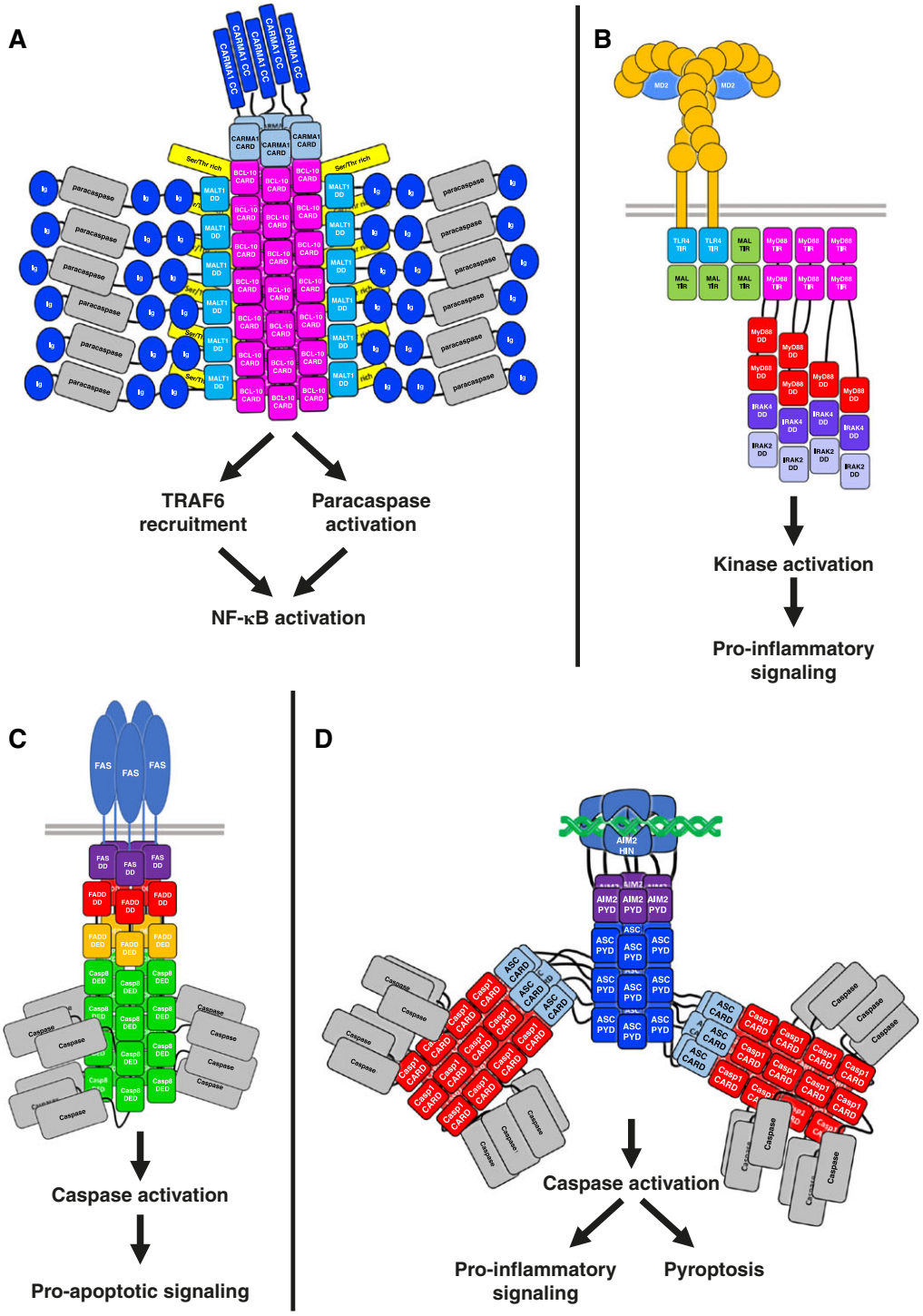

FIGURE 2 **Death-fold domain assemblies and their role as signaling platforms**. (A) Activation of CARMA1 by T cell (TCR) or B cell receptor (BCR) mediated phosphorylation results in oligomerization of CARMA1, possibly due to aggregation of coiled-coil domains, and nucleates the formation of BCL-10 filaments. Recruitment of MALT1 by BCL-10 leads to activation of the MALT1 paracaspase domain, recruitment, and oligomerization of TRAF6 to MALT1, and subsequent NF-κB signaling. Note: The C-terminal MAGUK domain of CARMA1 is not shown. (B) Recognition of PAMPs or DAMPs by TLRs is thought to induce dimerization of the cytoplasmic TLR TIR domains, which then serve as a recruitment platform for the TIR containing adaptor protein MAL. MAL subsequently recruits MyD88 through TIR:TIR domain interactions causing the MyD88 DDs to form a helical assembly with IRAKs through DD:DD interactions, and the resulting proximity based auto- and cross-phosphorylation of IRAKs leads to the activation of pro-inflammatory transcription factors, such as NF-κB and AP-1. For clarity, the IRAK kinase domains are not shown. (C) Activation of the FAS receptor recruits FADD via DD:DD interactions. The resulting clustering of FADD DEDs nucleates the formation of caspase-8 tDED assemblies, this in turn causes clustering, and subsequent proximity based activation of the procaspase. Activated caspase-8 is able to induce pro-apoptotic signaling through processing of procaspase-3. (D) Detection of cytoplasmic dsDNA by AIM2 results in clustering of the AIM2 PYD. The AIM2 PYD is thought to then recruit ASC via PYD:PYD interactions, forming a filamentous assembly. Formation of the ASC PYD filament initiates clustering of the ASC CARDs and subsequent recruitment of procaspases through CARD:CARD interactions leads to caspase activation and signaling

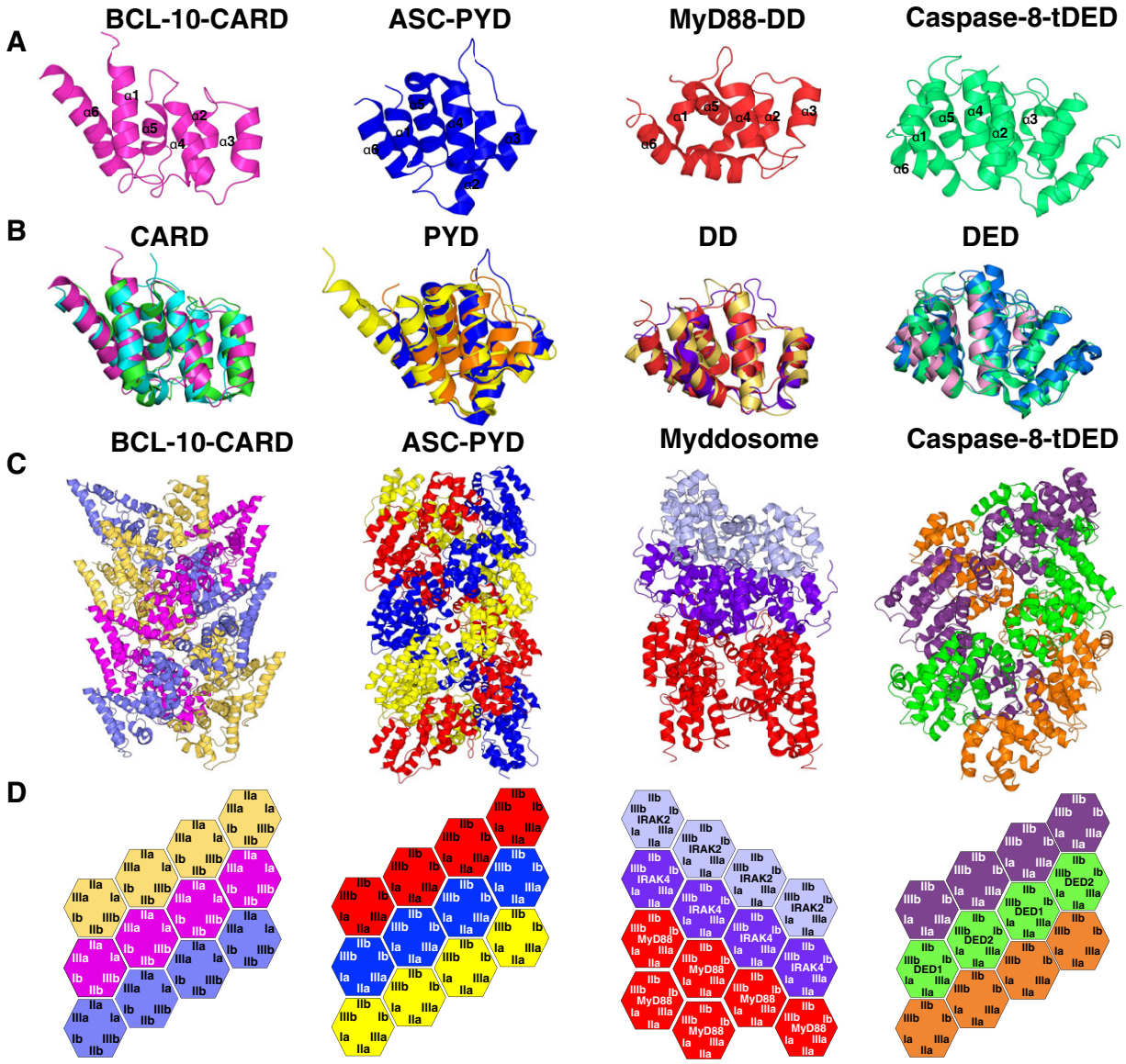

FIGURE 3 **Structural features of death-fold domains and their assemblies.** (A) Structures of BCL-10 CARD (PDB ID 6BZE), ASC PYD (PDB ID 3J63), MyD88 DD (PDB ID 3MOP), and caspase-8 tDED (PDB ID 5L08). (B) Superposition of CARDs from BCL-10 (pink; PDB ID 6BZE), Apaf-1 (cyan; PDB ID 5WVC), and MAVS (green; PDB ID 3J6J), PYDs from ASC (blue; PDB ID 3J63), AIM2 (yellow; PDB ID 3VD8), and NLRP3 (orange; PDB ID 3QF2), DDs from MyD88 (red; PDB ID 3MOP), IRAK4 (purple; PDB ID 3MOP), and FADD (gold; PDB ID 3OQ9), DED from PEA15 (pink; PDB ID 2LS7), and tDEDs from caspase-8 (green; PDB ID 5L08) and MC159 (blue; PDB ID 2F1S). (C) Representation of the BCL-10-CARD (PDB ID 6BZE), ASC-PYD (PDB ID 3J63), Myddosome (PDB ID 3MOP), and caspase-8 tDED (PDB ID 5L08) assemblies. The assemblies form through the type I, II, and III interfaces common among DF assemblies. (D) Schematic diagram of the type I, II, and III interactions of the BCL-10-CARD, ASC-PYD, Myddosome, and caspase-8 tDED assemblies. Note: Caspase-8 tDED units represented in purple and orange alternate between DED1 and DED2

other DF domains, DEDs contain a surface-exposed hydrophobic patch formed predominantly by residues on helix H2, and a E/D-RxDL-motif, with the N-terminal acidic residue contributed by helix H2, and the C-terminal motif by helix H6. Also, tDEDs have an additional helix H7 at the C-terminus of DED1, linking DED1 to the second DED (DED2).[47,50–52] The DEDs of FADD and cFLIP, and tDEDs of procaspase-8 have been shown to form filamentous assemblies *in vitro*.[49] Comparison of the cryo-EM structure of procaspase-8 tDED assembly with the crystal structure suggests that the tDEDs undergo little to no conformational changes upon oligomerization.[49,50] FADD DED filaments may act as a template for helical association of procaspase-8 tDED in a mechanism similar to that reported for RIG-I: 'mitochondrial antiviral-signaling protein' (MAVS), and 'melanoma differentiation associated gene 5' (MDA5):MAVS assemblies (see below) (Fig. 2). The viral FLIP MC159 inhibits the concentration-dependent, proximity-based auto-activation of caspase-8 by binding to the procaspase-8 tDED and preventing further oligomerization.[49,50]

2.3 | The CARD subfamily

The CARD subfamily (Fig. 1) was first identified in the apoptotic signaling proteins RAIDD, caspase-2, and 'cell death protein 3' (CED-3), an orthologue of caspase-9, due to sequence similarity and their known involvement in apoptotic signaling.[53] Originally described

as a motif that facilitated the recruitment of caspases to an apoptotic signaling complex, CARD-containing proteins are now known to have a broad range of functions in multiple immune system signaling pathways. The roles of CARDs can be broadly classified into 3 groups: the CARDs found as pro-domains of caspases, CARDs that act as receptors or adaptors in the assembly of signaling complexes, and CARDs that inhibit or otherwise modulate signaling complexes.

The CARD-containing proteins 'apoptotic protease activating factor-1' (Apaf-1),[54] RIG-I,[9,55] and 'NLR family CARD domain-containing protein 4' (NLRC4), serve as recruitment domains for downstream adaptor proteins or caspases following activation of the receptors' pattern recognition domain (e.g a leucine-rich repeat domain or WD repeat domain) by PAMP or DAMP ligands such as mitochondrial cytochrome c, viral genomic material, or bacterial flagellin. Adaptor proteins such as ASC, which contains both an N-terminal PYD and a C-terminal CARD,[12] act to link the PYD-containing receptor proteins to caspase recruitment and amplify receptor signaling due to homotypic interactions, with subsequent recruitment, oligomerization, and activation of CARD containing procaspases through CARD:CARD interactions (Fig. 2).

The 'CARD-coiled coil' (CARD-CC) containing proteins, including 'caspase-recruitment domain membrane-associated guanylate kinase (MAGUK) protein' (CARMA) 1–3 and CARD9, nucleate the formation of the CBM complexes, typically upon T- or B-cell receptor, natural killer cell receptor, or dectrin-induced phosphorylation of the CARD-CC by protein kinase C.[56–59] In the prototypical CBM, phosphorylation of CARMA1, which is thought to reside in an auto-inhibited state, activates CARMA1, which in turn recruits 'B-cell lymphona 10' (BCL-10) and nucleates the formation of filamentous BCL-10 assemblies. The CARD-CC proteins CARMA 1–3 contain an N-terminal CARD, central CC domain, and C-terminal MAGUK domain, while CARD9 lacks the MAGUK domain, containing only an N-terminal CARD and C-terminal CC domain. Recruitment of BCL-10, which contains an N-terminal CARD and C-terminal Ser/Thr-rich domain, occurs via CARD:CARD interactions with CARMA1. The paracaspase, 'mucosa-associated lymphoid tissue lymphoma translocation protein 1' (MALT1), is recruited to the CARMA1/BCL-10 complex through interactions between the CARD and the Ser/Thr-rich domain of BCL-10 and the N-terminal DD and central 'immunoglobulin' (Ig) domains (Ig1 and Ig2) of MALT1 (Fig. 2). The recruited MALT1 rapidly dimerizes, leading to paracaspase activation, recruitment and oligomerization of TRAF6, induction of TRAF6 ubiquitin ligase activity, and subsequent NF-κB activation.[19,20,60,61]

The structures of several CARDs have been determined in isolation by various methods, and display the 6-helical bundle fold characteristic of the DF superfamily. A feature that appears unique for the DF of CARDs is the morphology of helix α1, which is often kinked or separated into 2 separate helices.[54,62,63] As with all members of the DF superfamily, the orientations and lengths of several helices often differ among the individual CARDs, and presumably confer some degree of specificity for the binding partners of CARD-containing proteins. Notably, RIG-I, MDA5, and NOD2 contain 'tandem CARDs' (tCARDs) located sequentially at the N-terminus of the protein.[9,55,64]

In addition to the structures of CARDs solved in isolation, the CARDs of Apaf-1,[54,63] procaspase-1,[65] BCL-10,[19] MAVS,[9] NLRC4, and RIG-I[66] have been determined in reconstituted signaling assemblies that mimic those formed *in vivo*. The crystal structures of the RIG-I tCARDs[66] and the cryo-EM structure of a filament of MAVS CARDs[9] and procaspase-1 CARDs[65] reveal that the CARDs of these proteins have the ability to form helical assemblies similar to those of the DD assemblies. Unlike MAVS and caspase CARD filaments, which form continuous open-ended assemblies, the RIG-I tCARD assembly is limited to that of a tetramer of tCARDs. A helical rise half the height of the tCARD subunit sterically prohibits the incorporation of further subunits, resulting in a structure resembling a lock-washer (or split-washer). The structure of a tetramer of RIG-I tCARDs in complex with 4 MAVS CARDs reveals that the split-washer assembly of RIG-I tCARDs serves as a template for the formation of MAVS CARD filaments, by recruiting MAVS CARDs along the same helical trajectory as the RIG-I tCARD assembly.[9]

Following nucleation of MAVS CARD filaments by RIG-I, MAVS TRAF-binding sites cluster to recruit TRAF proteins and activate downstream signaling.[9] The structure of the 'NLR family apoptosis inhibitory protein 5' (NAIP5):NLRC4 signalosome suggests that upon binding of flagellin by NAIP5, NLRC4 is recruited to the assembly and further recruits additional NLRC4 molecules. The NAIP5:NLRC4 assembly resembles a wheel-like structure, with the N-terminal CARDs positioned into close proximity within the center of the structures. In a mechanism similar to RIG-I:MAVS assemblies, the NAIP5:NLRC4 CARDs are likely to form a helical template that serves to recruit ASC or procaspase-1 via homotypic CARD interactions.[10,67,68]

2.4 | The PYD subfamily

There are at least 23 human and 30 mouse genes that encode PYD-containing proteins. The best characterized of these are the DNA-sensing 'absent in melanoma 2' (AIM2), a member of the PYHIN family, that contains an N-terminal PYD and a C-terminal HIN domain,[69] the adaptor protein ASC, which is comprised of an N-terminal PYD and C-terminal CARD,[12,30,70,71] and the PRR 'NLR family PYD containing protein 3' (NLRP3), which contains an N-terminal PYD, a central NOD, and a C-terminal 'leucine rich repeat domain' (LRR)[72] (Fig. 1). AIM2 and NLRP3 have been shown to form large assemblies termed inflammasomes.[12,70] Activation of either NLRP3 or AIM2 and related 'AIM2-like receptors' (ALRs) is typically followed by the recruitment of ASC via homotypic interactions between the N-terminal PYD of ASC and the PYDs of the PRR. The recruited ASC forms helical filaments through PYD:PYD interactions, and in turn recruits procaspases and nucleates the formation of procaspase filaments, through either CARD:CARD interactions, as in the case of procaspase-1, or PYD:DED interactions, as in the case of procaspase-8.[12,30,65,70,73]

The monomeric structures of the PYDs of AIM2,[69] ASC,[71] pyrin,[74] and various NLRPs have been determined by either nuclear magnetic resonance (NMR) or crystallography. In addition to the characteristic DF, PYDs display a short α3 helix and an elongated α2-α3 loop compared to other DF subfamilies. In the case of the ASC PYD, the acidic

conditions used for NMR spectroscopy appear to have abolished self-association, and thus provide little insight into the interfaces of the PYD assemblies. However, the cryo-EM structure of the ASC PYD filament at near-atomic resolution demonstrates that few conformational changes are apparent between monomeric PYD and those of the filament. In the filament, the α3 helix and α2-α3 loops appear to be stabilized by the type I, II, and III interfaces. The ASC PYD filaments display a 3-fold helical symmetry, when looking down the helical axis, featuring a hollow center with an inner diameter of ~ 20 Å and outer diameter of ~90 Å.[12] The crystal structure of the AIM2 PYD displays little difference to that of the ASC and NLRP3 PYDs, with the exception of the α1 and α6 helices, which are elongated in the AIM2 PYD.[12,69,72] PYDs typically display highly positively or negatively charged surface regions, which are either involved in self-association or conferring specificity for a particular binding partner.[12,69]

2.5 | Death-fold family oligomerization interfaces

The DF domains display 3 shared asymmetric non-overlapping interfaces that can potentially interact with up to 6 different binding partners (Fig. 3). The interfaces between layers or strands of the DF assemblies may differ depending on the symmetry or oligomerization pattern used to describe the assembly, for instance the Myddosome[42] and procaspase-1 CARD assemblies[65] have been described as left-handed helices with the type III interface composed of intrastrand interactions, while the ASC PYD filament has been described as a 3-stranded right-handed assembly with intrastrand interactions mediated by the type I interface.[12] However the interfaces remain relatively conserved among DF family members.[12,42,45]

The type I interfaces form between helices H1 and H4 (interface Ia) of one DF domain and H2 and H3 (interface Ib) of an adjacent domain, and are largely composed of electrostatic interactions. The type II interaction is formed between residues of helix H4 (IIa) of one DF domain and residues of the loop region between helices H5 and H6 of another. Finally, the type III interaction is formed between helix H3 (IIIa) of one DF domain and the 2 loop regions connecting helices H1 and H2, and helices H3 and H4, respectively (patch IIIb) of the other DF domain.[12,42,45] The procaspase-8 tDEDs differ slightly from this arrangement as within each tDED, the type Ib surface of the first DED (DED1) interacts with the type Ia surface of the second DED (DED2). Furthermore, the type I interface of the tDED filament is predominantly mediated by hydrophobic interactions, whereas the type II and III interactions are complementary electrostatic interactions.[49]

3 | TIR DOMAINS

The TIR domain is a small globular domain consisting of 125–150 residues, and in animals and plants it is usually found in multidomain proteins involved in innate immunity pathways (Fig. 1). Many bacterial proteins also contain TIR domains, and at least some of them are associated with virulence by suppressing host innate immunity signaling pathways.

In mammals TIR domains are found (i) on the cytosolic side of TLRs, which recognize a wide variety of PAMPs and DAMPs either at the cell surface or in the endosomes, and trigger activation of NF-κB and IFN regulatory factor (IRF) transcription factors to induce cytokine production[75]; (ii) on the cytosolic side of Interleukin-1 receptors (IL–1Rs), which regulate the activities of the IL-1 family of proinflammatory cytokines[76]; (iii) in the cytosolic signaling adaptor molecules MyD88, MAL, 'TIR domain-containing adaptor protein inducing IFN-β' (TRIF), and 'TRIF-related adaptor molecule' (TRAM), which are recruited to TLRs and IL-1Rs (only MyD88) via TIR:TIR domain interactions upon activation by PAMP/DAMP or cytokine recognition[77]; (iv) in 'sterile-α and TIR motif-containing protein' (SARM), which was first described as an adaptor protein involved in regulation of TLR signaling,[78] but has more recently been established as an executioner of neuronal cell-death following insults such as oxygen and glucose deprivation, axonal degeneration following nerve transection and vincristine treatment[79,80]; and (v) in 'B-cell adaptor for phosphoinositide 3-kinase' (BCAP), which has recently been proposed to be the sixth TIR domain-containing TLR adaptor, linking phosphoinositide metabolism with negative regulation of TLR pathways.[81,82]

In plants, TIR domains are the signaling component of a major subclass of disease resistance proteins that recognize pathogen effector proteins introduced into the plant cell during the invasion of the plant. These proteins are typically referred to as plant NLRs, based on their similarity to mammalian NLRs, and they trigger defense responses that often include localized cell death at the site of infection.[26] Self-association of these receptors via TIR:TIR interactions is critical for activation of defense responses.

A wide range of both pathogenic and nonpathogenic bacterial species also have TIR domain-containing proteins.[83,84] Some of these proteins such as TcpB from *Brucella melitensis* and TcpC from uropathogenic *Escherichia coli* CFT073 have been shown to supress TLR signaling in mammals by interfering with receptor–adaptor TIR domain interactions.[85,86]

'Similar expression to fibroblast growth factor genes and IL-17R' (SEFIR) domains, which in mammals are present in both the cytosolic segment of IL-17Rs and in the cytosolic adaptor protein 'NF-κB activator 1' (ACT1), share similarity with TIR domains, and these 2 domain families have been classified as the STIR (SEFIR/TIR) domain superfamily.[87] Analogous to the role of TIR domains in TLR and IL-1R signaling, Act1 is recruited to IL-17R complexes via SEFIR:SEFIR interactions upon ligand stimulation.[88] SEFIR domains are also found in bacterial proteins, but their functions are not known.[89]

3.1 | TIR and SEFIR domain structure

TIR and SEFIR domains have a flavodoxin-like fold, consisting of a central 5-stranded parallel β-sheet surrounded by 4–7 α-helices on both sides of the sheet. The secondary elements and loops are labeled sequentially; for example, the AB loop connects helix αA and strand βB, while the BB loop connects strand βB and helix αB. TIR domain structures are available for the human TLRs 1, 2, 6, and 10[90,92]; the human TLR adaptors MyD88, MAL, TRAM, TRIF, and BCAP[5,81,86,93–95,97–99]; human 'IL-1R accessory protein-like 1' (IL-1RAPL)[100]; the Toll-related

receptor TRR-2 from the lower metazoan *Hydra magnipapillata* (PDB ID 4W8G and 4W8H); the flax NLR protein L6[101]; the Arabidopsis NLR proteins RPS4, RRS1, SNC1, and RPP1[27,102]; the Arabidopsis protein AtTIR[103]; the grape NLR protein RPV1[104]; the *Paracoccus denitrificans* protein PdTIR,[105] and the *Brucella melitensis* virulence factor TcpB.[85,96,97]

In addition, SEFIR domain structures are available for the human IL-17RA and IL-17RB receptors[106,107] and the *Bacillus cereus* protein BcSEFIR.[108] The structural core of all TIR domains are conserved but there are significant structural differences in the surrounding loops and α-helices (size, number, and orientation), in particular between the different sub-types of TIR domains (TLRs, TLR-adaptors, IL-1Rs, plant, and bacteria) (reviewed in [109]). For example, in plant TIR domains the region between the βD and βE strands contains 3 well-defined helices (αD1, αD2, and αD3) and is significantly different compared to both mammalian and bacterial TIR domains, which only contain 1 or 2 short helices (Fig. 4A). The central 5-stranded β sheet of SEFIR domains as well as the 3 helices αA, αB, and αE superimpose well with the TLR receptor TIR domains, but there are significant structural differences in the CC region, the αC and αD helices, and the DD region (Fig. 4A).

3.2 | TIR domain assemblies

PAMP or DAMP recognition by TLRs drives the intracellular TIR domains to self-associate and subsequently recruit TIR domain-containing adaptor proteins via homotypic TIR-domain interactions to initiate signaling. Although structures are available for many receptor and adaptor TIR domains, the molecular mechanisms underpinning adaptor recruitment to TLRs via homotypic TIR-domain interactions have remained controversial, due to the difficulty of reconstituting stable TIR domain oligomers (reviewed in [3]). Our studies of MAL and MyD88-dependent TLR4 signaling using electron microscopy and *in vitro* reconstitution assays[5] revealed that the TIR domain of MAL can (i) self-assemble or assemble with the TLR4 TIR domain into filaments, and (ii) nucleate large crystalline assemblies of the MyD88 TIR domain. Both the MAL filament and the MyD88 assembly consist of proto-filaments containing 2 parallel strands of TIR-domain subunits in a head-to-tail arrangement, mediated by the highly conserved BB loop (links the βB-strand to the αB-helix), which has previously been shown to be critical for TLR signaling (Fig. 4B). Although similar-scale TIR-domain assemblies are unlikely to form in the cell during a normal signaling event, the MAL and MyD88 TIR-domain proto-filament structures reflect the molecular mechanisms of TIR:TIR interactions during this process: binding of lipopolysaccharide (LPS) to TLR4 causes the dimerization of its TIRs, which provides a platform for MAL to start an open-ended assembly, which in turn nucleates an open-ended assembly of MyD88 TIRs. Consistent with this model, Latty et al.[110] recently demonstrated, using live cell imaging of macrophages, that TLR4 assembles into dimers upon LPS stimulation, which rapidly nucleates formation of MyD88 assemblies consisting of 6 or 12 subunits. Several of the residues in the TIR:TIR interfaces in the MAL and MyD88 proto-filaments are highly conserved in mammalian TIR domains, suggesting that this may be a general mechanism of assembly formation in both TLR and IL-1R signaling.

Structures of plant TIR domains involved in effector-triggered immunity have revealed 2 functionally relevant TIR:TIR domain interactions that involve highly conserved residues: the DE interface, which involves residues from the αD, βE, and αE regions, found important for signaling by the L6 NLR from flax[101]; and the AE interface, which involves residues from αA, αE, and the AA and EE loops, found critical for RPS4-mediated signaling in Arabidopsis[102] and RPV1-dependent signaling in the wild grapevine *Muscadinia rotundifolia*.[104] These 2 interfaces are symmetric and different to the asymmetric interactions observed in the MAL and MyD88 proto-filaments, suggesting that the TIR-domain fold may have evolved to mediate different types of homotypic interactions (Fig. 4B). Recent structure-function studies of TIR domains from the SNC1 and RPP1 R proteins[27] demonstrated that both AE and DE interactions control self-association and are required for triggering an immune response. The SNC1 crystal structure also revealed an extended TIR domain superhelix propagated through the AE and DE interfaces, which may facilitate SCAF in plant cell-death signaling (Fig. 4B).

The available crystal structures of bacterial TIR domains, PdTIR from the nonpathogenic *Paracoccus denitrificans* and TcpB from the pathogenic *Brucella melitensis*, reveal a common symmetric self-association interface distinct from the plant TIR domains, which involves residues in the DD and EE loops.[85,96,97,105] The BB loops from the 2 interacting molecules are exposed to the solvent for possible interaction with host molecules.

Common interaction interfaces have not yet been reported for SEFIR domains, but functional analyses have identified helix αC as a critical structural motif for heterotypic SEFIR:SEFIR interactions between Act1 and IL-17RA/IL-17RB while the αB helix of Act1 is important for homotypic interactions between Act1 SEFIR domains.[106,107]

3.3 | TIR domain enzyme activity

SARM has been shown to have TLR-independent roles in neurons,[79,80] and the local cell death program induced by SARM after axonal injury involves rapid breakdown of 'nicotinamide adenine dinucleotide' (NAD^+) into nicotinamide and ADP-ribose.[111] Enforced dimerization of the C-terminal TIR domain of SARM is sufficient to cause depletion of axonal NAD^+ and induce axonal degeneration in the absence of injury,[79] and Essuman et al.[112] recently demonstrated that the SARM TIR domain has intrinsic NADase activity and suggested it shares similarities to nucleotide hydrolases and nucleoside transferases. The TLR4 and MyD88 TIR domains did not show NADase activity, suggesting this activity is a unique feature of SARM. Essuman et al.[112] also showed that a glutamate residue, E642, in the predicted αC helix of SARM TIR is critical for the NADase activity. An equivalent glutamate residue is not found in TLR and IL-1R receptor and adaptor TIR domains in mammals, but it is conserved in many bacterial and plant TIR domains, and in a second paper by Essuman et al.,[113] it was confirmed that several of the bacterial TIR domains also have NADase activity. For both SARM and the bacterial proteins, clustering of the TIR domains on beads was required for NADase activity, suggesting that TIR domain self-association may be a requirement for enzymatic

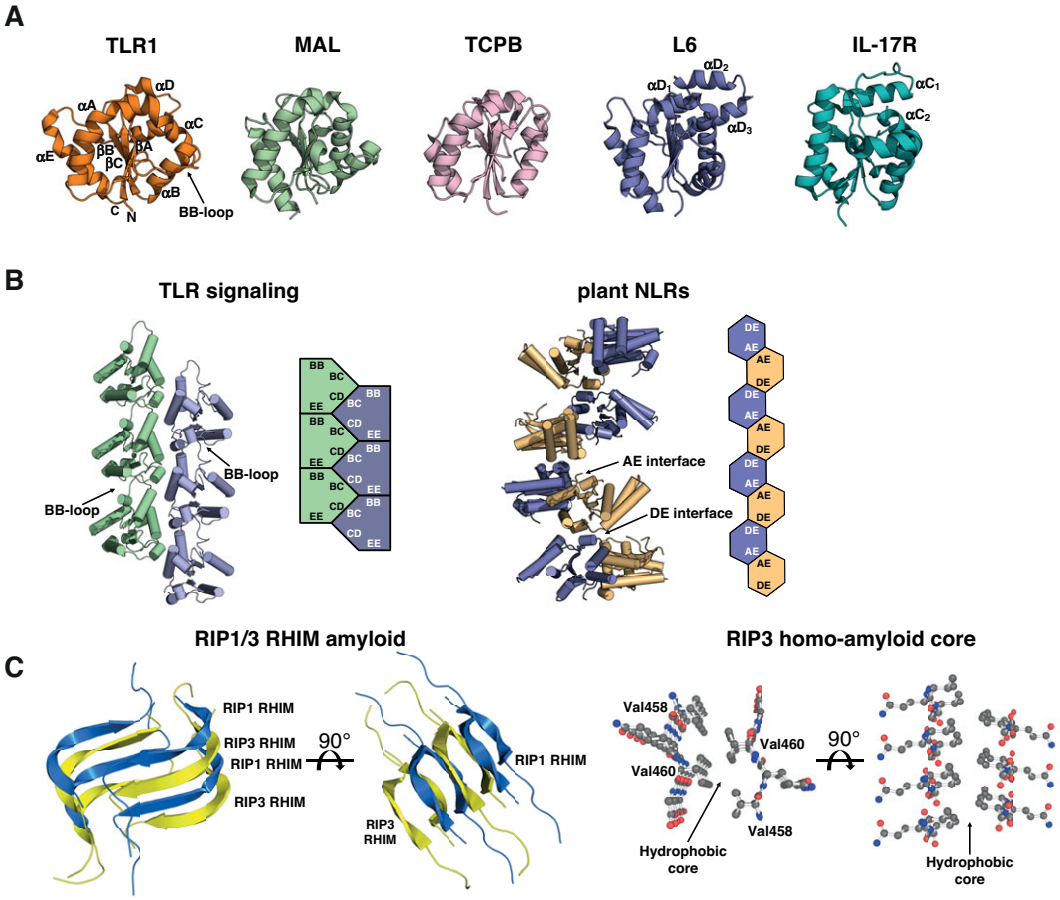

FIGURE 4 **Structural features of TIR and SEFIR domains, and RHIM regions and their assemblies.** (A) Structures of human TLR1 (PDB ID 1FYV), human MAL (PDB ID 5UZB), *Brucella melitensis* TcpB (PDB ID 4C7M) and flax L6 (PDB ID 3OZI) TIR domains and the human IL-17RA (PDB ID 4NUX) SEFIR domain. The structures are shown in analogous orientations and unique structural elements are highlighted. (B) Left panel: Cartoon representation of the MAL TIR domain proto-filament (PDB ID 5UZB). The assembly consists of 2 parallel strands of TIR-domain subunits in a BB-loop-mediated head-to-tail arrangement. The schematic diagram highlights the assembly interfaces: BB surface, BB loop; EE surface, βD, βE strands, and αE helix; BC surface, αB and αC helices; CD surface, αD helix and CD loop. Right panel: Cartoon representation of a hypothetical assembly of plant TIR domains utilizing the symmetric AE and DE interfaces observed in the SNC1 crystal structure (PDB ID 5TEC). The schematic diagram highlights the assembly interfaces: AE surface, αA and αE helices; DE surface, αD_1 and αE helices and connecting loops. (C) The structure of the RIP1:RIP3 RHIM domain hetero-amyloid (PDB ID 5V7Z). Strands of the amyloid are formed by alternating RHIM domains aligned forming 2 parallel β-sheets; the 2 β-sheets are arranged in an antiparallel fashion and form a hydrophobic core. The hydrophobic core is clearly visible in the crystal structure of the RIP3 homo-amyloid (PDB ID 5ZCK)

activity. Interestingly, the Act1 SEFIR domain has recently been shown to directly bind and stabilize mRNAs encoding key inflammatory proteins,[114] suggesting that nucleotide binding may be a common feature among TIR and SEFIR domains.

4 | RHIM REGIONS

The 'RIP homotypic interaction motif' (RHIM) is a short sequence of ~15–20 amino acids, first identified as a homotypic interaction motif that facilitates association between RIP1 and RIP3.[115] Located at the C-terminus of RIP3 and adjacent to the C-terminal DD in RIP1, the RHIM domain forms the core of the amyloid signaling complex known as the necrosome, which coordinates necroptosis, a regulated form of necrosis that occurs upon inhibition of caspase-8 mediated apoptosis.[16,115–117] The RHIM region contains a core motif of (V/I)-Q-(V/I/L/C)-G, and is also found in 'DNA-dependent activator of IFN regulatory factors' (DAI),[118] TRIF,[119,120] mouse cytomegalovirus 'viral inhibitor of RIP activation' (vIRA),[121] 'herpes simplex virus' (HSV)-1 ICP6 and HSV-2 ICP10,[122] and shares similarities with the amyloid-forming domain of the fungal protein HET-s.[123] Necroptosis appears to be activated when recruitment of RIP1 by either TNFR1 or TRIF fails to result in caspase-8 activation, thus sparing the cell from apoptosis. In the absence of apoptosis, RIP1 and RIP3 associate via their RHIM domains, forming an amyloid fibril; oligomerization and subsequent activation of RIP3 leads to the recruitment and phosphorylation of 'mixed lineage kinase domain-like protein (MLKL) via the N-terminal kinase domain of RIP3, triggering MLKL oligomerization,

recruitment to the plasma membrane and cell death, presumably by permeabilization of the membrane or disruption of membrane homeostasis.[16,18,116,117,124–127]. In addition to RIP1-mediated necroptosis, TRIF and DAI have been reported to recruit RIP3, resulting in MLKL activation and necroptosis independent of RIP1,[118–120] while ICP6 and ICP10 appear to interact with RIP1 and RIP3 and disrupt necroptosis in a RHIM-dependent manner.[122]

Structures of the RHIM regions are limited to the crystal structure of a homo-amyloid formed by the RIP3 tetrad VQVG and the solid-state NMR structure of the RIP1/RIP3 hetero-amyloid complex (Fig. 4C).[18] Both the RIP3 homo-amyloid and RIP1/RIP3 hetero-amyloid fibril feature two parallel β-sheets arranged together in an anti-parallel fashion, with the hydrophobic residues of the (V/I)-Q-(V/I/L/C)-G tetrad forming a hydrophobic core. The overall structure of the RIP1:RIP3 hetero-amyloid complex further reveals that each strand in the parallel β-sheet is broken into 4 short β-strand segments separated by short turns. In the RIP1:RIP3 hetero-amyloid fibril, the parallel strands of the β-sheets are formed from alternating RIP1:RIP3 RHIM domains. In addition to the hydrophobic core, stacking of the parallel RIP1:RIP3 RHIM domains is supported by Asn and Gln ladders formed between the side chains of Asn535 in RIP1 and Asn454 in RIP3 and the side chains of RIP1 residue Gln540 and RIP3 residue Gln459. Additional interactions including tyrosine stacking interactions formed between Tyr534 (RIP1) and Tyr453 (RIP3), and a Ser536 (RIP1)/Cys455 (RIP3) ladder further stabilize the assembly.[18]

5 | CONCLUDING REMARKS

In innate immunity and cell-death pathways, SCAF is emerging as a key signaling mechanism. The first characterized examples of SCAF involved members of the DF superfamily, but more recently RHIM regions and TIR domains have also been shown to form open-ended assemblies and to engage in SCAF. The higher order assemblies formed by these domains have distinct properties. The RHIM assemblies resemble amyloids and prions, in which adjacent interacting elements are tightly packed, resulting in cooperative contacts and a high barrier of dissociation. The DF signalosomes consist of folded domains, but cooperative interactions among 6 weakly associating adjacent surfaces lead to assemblies that can be as stable as amyloids.[8,12] By contrast, the 2-stranded head-to-tail assemblies of TIR domains have lower valency and are less stable. The MAL filament, for example, disassembles at low temperatures in solution.[3] The static and dynamic properties associated with the different assemblies could be directly related to the function of the assemblies and the biological outcome of the signaling pathways they are involved in. For example, in TLR signaling, it is likely that the low valency and observed dynamic properties of TIR domain assemblies are important for the observed rapid assembly and disassembly of TLR4:MAL:MyD88 complexes in macrophages.[110] On the other hand, DF and RHIM assemblies may persist even after cell lysis.

AUTHORSHIP

J.N, B.K, and T.V wrote and edited the manuscript.

ACKNOWLEDGMENTS

The work in the authors' laboratories was supported by the National Health and Medical Research Council (NHMRC grants 1107804, 1071659, and 1003326). B.K. is an NHMRC Principal Research Fellow (1003325, 1110971), and T.V. is funded by an Australian Research Council Discovery Early Career Research Award (DE170100783).

DISCLOSURE

The authors declare no conflicts of interest.

REFERENCES

1. Hauenstein AV, Zhang L, Wu H. The hierarchical structural architecture of inflammasomes, supramolecular inflammatory machines. *Curr Opin Struct Biol*. 2015;31:75–83.
2. Kagan JC, Magupalli VG, Wu H. SMOCs: supramolecular organizing centres that control innate immunity. *Nat Rev Immunol*. 2014;14:821–826.
3. Nimma S, Ve T, Williams SJ, Kobe B. Towards the structure of the TIR-domain signalosome. *Curr Opin Struct Biol*. 2017;43:122–130.
4. Vajjhala PR, Ve T, Bentham A, Stacey KJ, Kobe B. The molecular mechanisms of signaling by cooperative assembly formation in innate immunity pathways. *Mol Immunol*. 2017;86:23–37.
5. Ve T, Vajjhala PR, Hedger A, et al. Structural basis of TIR-domain-assembly formation in MAL- and MyD88-dependent TLR4 signaling. *Nat Struct Mol Biol*. 2017;24:743–751.
6. Wu H. Higher-order assemblies in a new paradigm of signal transduction. *Cell*. 2013;153:287–292.
7. Yin Q, Fu TM, Li J, Wu H. Structural biology of innate immunity. *Annu Rev Immunol*. 2015;33:393–416.
8. Hou F, Sun L, Zheng H, Skaug B, Jiang QX, Chen ZJ. MAVS forms functional prion-like aggregates to activate and propagate antiviral innate immune response. *Cell*. 2011;146:448–461.
9. Wu B, Peisley A, Tetrault D, et al. Molecular imprinting as a signal-activation mechanism of the viral RNA sensor RIG-I. *Mol Cell*. 2014;55:511–523.
10. Xu H, He X, Zheng H, et al. Structural basis for the prion-like MAVS filaments in antiviral innate immunity. *Elife*. 2015;3:e01489.
11. Lu A, Li Y, Schmidt FI, et al. Molecular basis of caspase-1 polymerization and its inhibition by a new capping mechanism. *Nat Struct Mol Biol*. 2016;23:416–425.
12. Lu A, Magupalli VG, Ruan J, et al. Unified polymerization mechanism for the assembly of ASC-dependent inflammasomes. *Cell*. 2014;156:1193–1206.
13. Sborgi L, Ravotti F, Dandey VP, et al. Structure and assembly of the mouse ASC inflammasome by combined NMR spectroscopy and cryo-electron microscopy. *Proc Natl Acad Sci USA*. 2015;112:13237–13242.
14. He S, Liang Y, Shao F, Wang X. Toll-like receptors activate programmed necrosis in macrophages through a receptor-interacting kinase-3-mediated pathway. *Proc Natl Acad Sci USA*. 2011;108:20054–20059.
15. Kaiser WJ, Sridharan H, Huang C, et al. Toll-like receptor 3-mediated necrosis via TRIF, RIP3, and MLKL. *J Biol Chem*. 2013;288:31268–31279.
16. Li J, McQuade T, Siemer AB, et al. The RIP1/RIP3 necrosome forms a functional amyloid signaling complex required for programmed necrosis. *Cell*. 2012;150:339–350.

17. Meng H, Liu Z, Li X, et al. Death-domain dimerization-mediated activation of RIPK1 controls necroptosis and RIPK1-dependent apoptosis. *Proc Natl Acad Sci USA*. 2018;115:E2001–E2009.
18. Mompean M, Li W, Li J, et al. The structure of the necrosome RIPK1-RIPK3 core, a human hetero-amyloid signaling complex. *Cell*. 2018;173:1244–1253. e10.
19. David L, Li Y, Ma J, Garner E, Zhang X, Wu H. Assembly mechanism of the CARMA1-BCL10-MALT1-TRAF6 signalosome. *Proc Natl Acad Sci USA*. 2018;115:1499–1504.
20. Qiao Q, Yang C, Zheng C, et al. Structural architecture of the CARMA1/Bcl10/MALT1 signalosome: nucleation-induced filamentous assembly. *Mol Cell*. 2013;51:766–779.
21. Afonina IS, Van Nuffel E, Baudelet G, et al. The paracaspase MALT1 mediates CARD14-induced signaling in keratinocytes. *EMBO Rep*. 2016;17:914–927.
22. Blonska M, Lin X. CARMA1-mediated NF-kappaB and JNK activation in lymphocytes. *Immunol Rev*. 2009;228:199–211.
23. Che T, You Y, Wang D, Tanner MJ, Dixit VM, Lin X. MALT1/paracaspase is a signaling component downstream of CARMA1 and mediates T cell receptor-induced NF-kappaB activation. *J Biol Chem*. 2004;279:15870–15876.
24. Gross O, Gewies A, Finger K, et al. Card9 controls a non-TLR signalling pathway for innate anti-fungal immunity. *Nature*. 2006;442:651–656.
25. McAllister-Lucas LM, Ruland J, Siu K, et al. CARMA3/Bcl10/MALT1-dependent NF-kappaB activation mediates angiotensin II-responsive inflammatory signaling in nonimmune cells. *Proc Natl Acad Sci USA*. 2007;104:139–144.
26. Bentham A, Burdett H, Anderson PA, Williams SJ, Kobe B. Animal NLRs provide structural insights into plant NLR function. *Ann Bot*. 2017;119:827–702.
27. Zhang X, Bernoux M, Bentham AR, et al. Multiple functional self-association interfaces in plant TIR domains. *Proc Natl Acad Sci USA*. 2017;114:E2046–E2052.
28. Nanson JD, Rahaman MH, Ve T, Kobe B. Regulation of signaling by cooperative assembly formation in mammalian innate immunity signalosomes by molecular mimics. *Semin Cell Dev Biol*. 2018. https://doi.org/10.1016/j.semcdb.2018.05.002.
29. Nam YJ, Mani K, Ashton AW, et al. Inhibition of both the extrinsic and intrinsic death pathways through nonhomotypic death-fold interactions. *Mol Cell*. 2004;15:901–912.
30. Vajjhala PR, Lu A, Brown DL, et al. The inflammasome adaptor ASC induces procaspase-8 death effector domain filaments. *J Biol Chem*. 2015;290:29217–29230.
31. Schneider P, Thome M, Burns K, et al. TRAIL receptors 1 (DR4) and 2 (DR5) signal FADD-dependent apoptosis and activate NF-κB. *Immunity*. 1997;7:831–836.
32. Berglund H, Olerenshaw D, Sankar A, Federwisch M, McDonald NQ, Driscoll PC. The three-dimensional solution structure and dynamic properties of the human FADD death domain. *J Mol Biol*. 2000;302:171–188.
33. Huang B, Eberstadt M, Olejniczak ET, Meadows RP, Fesik SW. NMR structure and mutagenesis of the Fas (APO-1/CD95) death domain. *Nature*. 1996;384:638–641.
34. Cleveland JL, Ihle JN. Contenders in FasL/TNF death signaling. *Cell*. 1995;81:479–482.
35. Chinnaiyan AM, O'Rourke K, Yu GL, et al. Signal transduction by DR3, a death domain-containing receptor related to TNFR-1 and CD95. *Science*. 1996;274:990–992.
36. Hsu H, Shu H-B, Pan M-G, Goeddel DV. TRADD–TRAF2 and TRADD–FADD interactions define two distinct TNF receptor 1 signal transduction pathways. *Cell*. 1996;84:299–308.
37. Hsu H, Huang J, Shu H-B, Baichwal V, Goeddel DV. TNF-dependent recruitment of the protein kinase RIP to the TNF receptor-1 signaling complex. *Immunity*. 1996;4:387–396.
38. Hsu H, Xiong J, Goeddel DV. The TNF receptor 1-associated protein TRADD signals cell death and NF-κB activation. *Cell*. 1995;81:495–504.
39. Pobezinskaya YL, Liu Z. The role of TRADD in death receptor signaling. *Cell Cycle*. 2012;11:871–876.
40. Tinel A, Janssens S, Lippens S, et al. Autoproteolysis of PIDD marks the bifurcation between pro-death caspase-2 and pro-survival NF-κB pathway. *EMBO J*. 2007;26:197–208.
41. Park HH, Logette E, Raunser S, et al. Death domain assembly mechanism revealed by crystal structure of the oligomeric PIDDosome core complex. *Cell*. 2007;128:533–546.
42. Lin S-C, Lo Y-C, Wu H. Helical assembly in the MyD88–IRAK4–IRAK2 complex in TLR/IL-1R signalling. *Nature*. 2010;465:885.
43. Motshwene PG, Moncrieffe MC, Grossmann JG, et al. An oligomeric signalling platform formed by the toll-like receptor signal transducers MyD88 and IRAK4. *J Biol Chem*. 2009;284:25404–25411.
44. Ferrao R, Zhou H, Shan Y, et al. IRAK4 dimerization and trans-autophosphorylation are induced by Myddosome assembly. *Mol Cell*. 2014;55:891–903.
45. Wang L, Yang JK, Kabaleeswaran V, et al. The Fas–FADD death domain complex structure reveals the basis of DISC assembly and disease mutations. *Nat Struct Mol Biol*. 2010;17:1324.
46. Alcivar A, Hu S, Tang J, Yang X. DEDD and DEDD2 associate with caspase-8/10 and signal cell death. *Oncogene*. 2003;22:291.
47. Eberstadt M, Huang B, Chen Z, et al. NMR structure and mutagenesis of the FADD (Mort1) death-effector domain. *Nature*. 1998;392:941.
48. Hill JM, Vaidyanathan H, Ramos JW, Ginsberg MH, Werner MH. Recognition of ERK MAP kinase by PEA-15 reveals a common docking site within the death domain and death effector domain. *EMBO J*. 2002;21:6494–6504.
49. Fu T-M, Li Y, Lu A, et al. Cryo-EM structure of caspase-8 tandem DED filament reveals assembly and regulation mechanisms of the death-inducing signaling complex. *Mol Cell*. 2016;64:236–250.
50. Shen C, Yue H, Pei J, Guo X, Wang T, Quan J-M. Crystal structure of the death effector domains of caspase-8. *Biochem Biophys Res Commun*. 2015;463:297–302.
51. Yang JK, Wang L, Zheng L, et al. Crystal structure of MC159 reveals molecular mechanism of DISC assembly and FLIP inhibition. *Mol Cell*. 2005;20:939–949.
52. Muppidi J, Lobito A, Ramaswamy M, et al. Homotypic FADD interactions through a conserved RXDLL motif are required for death receptor-induced apoptosis. *Cell Death Differ*. 2006;13:1641.
53. Hofmann K, Bucher P, Tschopp J. The CARD domain: a new apoptotic signalling motif. *Trends Biochem Sci*. 1997;22:155–156.
54. Hu Q, Wu D, Chen W, et al. Molecular determinants of caspase-9 activation by the Apaf-1 apoptosome. *Proc Natl Acad Sci USA*. 2014;111:16254–16261.
55. Peisley A, Wu B, Xu H, Chen ZJ, Hur S. Structural basis for ubiquitin-mediated antiviral signal activation by RIG-I. *Nature*. 2014;509:110.
56. Matsumoto R, Wang D, Blonska M, et al. Phosphorylation of CARMA1 plays a critical role in T cell receptor-mediated NF-κB activation. *Immunity*. 2005;23:575–585.

57. Ruland J, Duncan GS, Wakeham A, Mak TW. Differential requirement for Malt1 in T and B cell antigen receptor signaling. *Immunity*. 2003;19:749–758.
58. Gross O, Gewies A, Finger K, et al. Card9 controls a non-TLR signalling pathway for innate anti-fungal immunity. *Nature*. 2006;442:651.
59. Gross O, Grupp C, Steinberg C, et al. Multiple ITAM-coupled NK-cell receptors engage the Bcl10/Malt1 complex via Carma1 for NF-κB and MAPK activation to selectively control cytokine production. *Blood*. 2008;112:2421–2428.
60. Li S, Yang X, Shao J, Shen Y. Structural insights into the assembly of CARMA1 and BCL10. *PLoS One*. 2012;7:e42775.
61. Sun L, Deng L, Ea C-K, Xia Z-P, Chen ZJ. The TRAF6 ubiquitin ligase and TAK1 kinase mediate IKK activation by BCL10 and MALT1 in T lymphocytes. *Mol Cell*. 2004;14:289–301.
62. Humke EW, Shriver SK, Starovasnik MA, Fairbrother WJ, Dixit VM. ICEBERG: a novel inhibitor of interleukin-1β generation. *Cell*. 2000;103:99–111.
63. Qin H, Srinivasula SM, Wu G, Fernandes-Alnemri T, Alnemri ES, Shi Y. Structural basis of procaspase-9 recruitment by the apoptotic protease-activating factor 1. *Nature*. 1999;399:549.
64. Fridh V, Rittinger K. The tandem CARDs of NOD2: intramolecular interactions and recognition of RIP2. *PLoS One*. 2012;7:e34375.
65. Lu A, Li Y, Schmidt FI, et al. Molecular basis of caspase-1 polymerization and its inhibition by a new capping mechanism. *Nat Struct Mol Biol*. 2016;23:416.
66. Peisley A, Wu B, Xu H, Chen ZJ, Hur S. Structural basis for ubiquitin-mediated antiviral signal activation by RIG-I. *Nature*. 2014;509:110–114.
67. Diebolder CA, Halff EF, Koster AJ, Huizinga EG, Koning RI. Cryoelectron tomography of the NAIP5/NLRC4 inflammasome: implications for NLR activation. *Structure*. 2015;23:2349–2357.
68. Hu ZH, Zhou Q, Zhang CL, et al. Structural and biochemical basis for induced self-propagation of NLRC4. *Science*. 2015;350:399–404.
69. Jin T, Perry A, Smith P, Jiang J, Xiao TS. Structure of the absent in melanoma 2 (AIM2) pyrin domain provides insights into the mechanisms of AIM2 autoinhibition and inflammasome assembly. *J Biol Chem*. 2013;288:13225–13235.
70. Dick MS, Sborgi L, Rühl S, Hiller S, Broz P. ASC filament formation serves as a signal amplification mechanism for inflammasomes. *Nat Commun*. 2016;7:11929.
71. de Alba E. Structure and interdomain dynamics of apoptosis-associated speck-like protein containing a CARD (ASC). *J Biol Chem*. 2009;284:32932–32941.
72. Oroz J, Barrera-Vilarmau S, Alfonso C, Rivas G, de Alba E. Asc Pyrin domain self-associates and binds Nlrp3 using equivalent binding interfaces. *J Biol Chem*. 2016;91:19487–19501.
73. Lu A, Li Y, Yin Q, et al. Plasticity in PYD assembly revealed by cryo-EM structure of the PYD filament of AIM2. *Cell Discov*. 2015;1:15013.
74. Vajjhala PR, Kaiser S, Smith SJ, et al. Identification of multifaceted binding modes for pyrin and ASC pyrin domains gives insights into pyrin inflammasome assembly. *J Biol Chem*. 2014;289:23504–23519.
75. Akira S, Uematsu S, Takeuchi O. Pathogen recognition and innate immunity. *Cell*. 2006;124:783–801.
76. Boraschi D, Italiani P, Weil S, Martin MU. The family of the interleukin-1 receptors. *Immunol Rev*. 2018;281:197–232.
77. Ve T, Gay NJ, Mansell A, Kobe B, Kellie S. Adaptors in toll-like receptor signaling and their potential as therapeutic targets. *Curr Drug Targets*. 2012;13:1360–1374.
78. Carty M, Goodbody R, Schroder M, Stack J, Moynagh PN, Bowie AG. The human adaptor SARM negatively regulates adaptor protein TRIF-dependent Toll-like receptor signaling. *Nat Immunol*. 2006;7:1074–1081.
79. Gerdts J, Summers DW, Sasaki Y, DiAntonio A, Milbrandt J. Sarm1-mediated axon degeneration requires both SAM and TIR interactions. *J Neurosci*. 2013;33:13569–13580.
80. Osterloh JM, Yang J, Rooney TM, et al. dSarm/Sarm1 is required for activation of an injury-induced axon death pathway. *Science*. 2012;337:481–484.
81. Halabi S, Sekine E, Verstak B, Gay NJ, Moncrieffe MC. Structure of the Toll/interleukin-1 receptor (TIR) domain of the B-cell adaptor that links phosphoinositide metabolism with the negative regulation of the Toll-like receptor (TLR) signalosome. *J Biol Chem*. 2017;292:652–660.
82. Troutman TD, Hu W, Fulenchek S, et al. Role for B-cell adapter for PI3K (BCAP) as a signaling adapter linking Toll-like receptors (TLRs) to serine/threonine kinases PI3K/Akt. *Proc Natl Acad Sci USA*. 2012;109:273–278.
83. Rana RR, Zhang M, Spear AM, Atkins HS, Byrne B. Bacterial TIR-containing proteins and host innate immune system evasion. *Med Microbiol Immunol*. 2013;202:1–10.
84. Spear AM, Loman NJ, Atkins HS, Pallen MJ. Microbial TIR domains: not necessarily agents of subversion?. *Trends Microbiol*. 2009;17:393–398.
85. Alaidarous M, Ve T, Casey LW, et al. Mechanism of bacterial interference with TLR4 signaling by Brucella Toll/interleukin-1 receptor domain-containing protein TcpB. *J Biol Chem*. 2014;289:654–668.
86. Snyder GA, Cirl C, Jiang J, et al. Molecular mechanisms for the subversion of MyD88 signaling by TcpC from virulent uropathogenic *Escherichia coli*. *Proc Natl Acad Sci USA*. 2013;110:6985–6990.
87. Novatchkova M, Leibbrandt A, Werzowa J, Neubuser A, Eisenhaber F. The STIR-domain superfamily in signal transduction, development and immunity. *Trends Biochem Sci*. 2003;28:226–229.
88. Wu L, Zepp J, Li X. Function of Act1 in IL-17 family signaling and autoimmunity. *Adv Exp Med Biol*. 2012;946:223–235.
89. Wu B, Gong J, Liu L, Li T, Wei T, Bai Z. Evolution of prokaryotic homologues of the eukaryotic SEFIR protein domain. *Gene*. 2012;492:160–166.
90. Jang TH, Park HH. Crystal structure of TIR domain of TLR6 reveals novel dimeric interface of TIR-TIR interaction for Toll-like receptor signaling pathway. *J Mol Biol*. 2014;426:3305–3313.
91. Nyman T, Stenmark P, Flodin S, Johansson I, Hammarstrom M, Nordlund P. The crystal structure of the human toll-like receptor 10 cytoplasmic domain reveals a putative signaling dimer. *J Biol Chem*. 2008;283:11861–11865.
92. Xu Y, Tao X, Shen B, et al. Structural basis for signal transduction by the Toll/interleukin-1 receptor domains. *Nature*. 2000;408:111–115.
93. Enokizono Y, Kumeta H, Funami K, et al. Structures and interface mapping of the TIR domain-containing adaptor molecules involved in interferon signaling. *Proc Natl Acad Sci USA*. 2013;110:19908–19913.
94. Lin Z, Lu J, Zhou W, Shen Y. Structural insights into TIR domain specificity of the bridging adaptor Mal in TLR4 signaling. *PLoS One*. 2012;7:e34202.
95. Ohnishi H, Tochio H, Kato Z, et al. Structural basis for the multiple interactions of the MyD88 TIR domain in TLR4 signaling. *Proc Natl Acad Sci USA*. 2009;106:10260–10265.
96. Kaplan-Turkoz B, Koelblen T, Felix C, et al. Structure of the Toll/interleukin 1 receptor (TIR) domain of the immunosuppressive Brucella effector BtpA/Btp1/TcpB. *FEBS Lett*. 2013;587:3412–3416.

97. Snyder GA, Deredge D, Waldhuber A, et al. Crystal structures of the Toll/interleukin-1 receptor (TIR) domains from the Brucella protein TcpB and host adaptor TIRAP reveal mechanisms of molecular mimicry. *J Biol Chem*. 2014;289:669–679.
98. Valkov E, Stamp A, Dimaio F, et al. Crystal structure of Toll-like receptor adaptor MAL/TIRAP reveals the molecular basis for signal transduction and disease protection. *Proc Natl Acad Sci USA*. 2011;108:14879–14884.
99. Hughes MM, Lavrencic P, Coll RC, et al. Solution structure of the TLR adaptor MAL/TIRAP reveals an intact BB loop and supports MAL Cys91 glutathionylation for signaling. *Proc Natl Acad Sci USA*. 2017;114:E6480–E9.
100. Khan JA, Brint EK, O'Neill LA, Tong L. Crystal structure of the Toll/interleukin-1 receptor domain of human IL-1RAPL. *J Biol Chem*. 2004;279:31664–31670.
101. Bernoux M, Ve T, Williams S, et al. Structural and functional analysis of a plant resistance protein TIR domain reveals interfaces for self-association, signaling, and autoregulation. *Cell Host Microbe*. 2011;9:200–211.
102. Williams SJ, Sohn KH, Wan L, et al. Structural basis for assembly and function of a heterodimeric plant immune receptor. *Science*. 2014;344:299–303.
103. Chan SL, Mukasa T, Santelli E, Low LY, Pascual J. The crystal structure of a TIR domain from *Arabidopsis thaliana* reveals a conserved helical region unique to plants. *Protein Sci*. 2010;19:155–161.
104. Williams SJ, Yin L, Foley G, et al. Structure and function of the TIR domain from the grape NLR protein RPV1. *Front Plant Sci*. 2016;7:1850.
105. Chan SL, Low LY, Hsu S, et al. Molecular mimicry in innate immunity: crystal structure of a bacterial TIR domain. *J Biol Chem*. 2009;284:21386–21392.
106. Zhang B, Liu C, Qian W, Han Y, Li X, Deng J. Crystal structure of IL-17 receptor B SEFIR domain. *J Immunol*. 2013;190:2320–2326.
107. Zhang B, Liu C, Qian W, Han Y, Li X, Deng J. Structure of the unique SEFIR domain from human interleukin 17 receptor A reveals a composite ligand-binding site containing a conserved alpha-helix for Act1 binding and IL-17 signaling. *Acta Crystallogr D Biol Crystallogr*. 2014;70:1476–1483.
108. Yang H, Zhu Y, Chen X, Li X, Ye S, Zhang R. Structure of a prokaryotic SEFIR domain reveals two novel SEFIR–SEFIR interaction modes. *J Struct Biol*. 2018;203:81–89.
109. Ve T, Williams SJ, Kobe B. Structure and function of Toll/interleukin-1 receptor/resistance protein (TIR) domains. *Apoptosis*. 2015;20:250–261.
110. Latty SL, Sakai J, Hopkins L, et al. Activation of Toll-like receptors nucleates assembly of the MyDDosome signaling hub. *ELife*. 2018;7:e31377.
111. Gerdts J, Brace EJ, Sasaki Y, DiAntonio A, Milbrandt J. SARM1 activation triggers axon degeneration locally via NAD(+) destruction. *Science*. 2015;348:453–457.
112. Essuman K, Summers DW, Sasaki Y, Mao X, DiAntonio A, Milbrandt J. The SARM1 Toll/interleukin-1 receptor domain possesses intrinsic NAD(+) cleavage activity that promotes pathological axonal degeneration. *Neuron*. 2017;93:1334–1343. e5.
113. Essuman K, Summers DW, Sasaki Y, et al. TIR domain proteins are an ancient family of NAD(+)-consuming enzymes. *Curr Biol*. 2018;28:421–430. e4.
114. Herjan T, Hong L, Bubenik J, et al. IL-17-receptor-associated adaptor Act1 directly stabilizes mRNAs to mediate IL-17 inflammatory signaling. *Nat Immunol*. 2018;19:354–365.
115. Sun X, Yin J, Starovasnik MA, Fairbrother WJ, Dixit VM. Identification of a novel homotypic interaction motif required for the phosphorylation of RIP (receptor interacting protein) by RIP3. *J Biol Chem*. 2001;277:9505–9511.
116. Cho Y, Challa S, Moquin D, et al. Phosphorylation-driven assembly of the RIP1-RIP3 complex regulates programmed necrosis and virus-induced inflammation. *Cell*. 2009;137:1112–1123.
117. Meng H, Liu Z, Li X, et al. Death-domain dimerization-mediated activation of RIPK1 controls necroptosis and RIPK1-dependent apoptosis. *Proc Natl Acad Sci USA*. 2018:201722013.
118. Upton JW, Kaiser WJ, Mocarski ES. DAI/ZBP1/DLM-1 complexes with RIP3 to mediate virus-induced programmed necrosis that is targeted by murine cytomegalovirus vIRA. *Cell Host Microbe*. 2012;11:290–297.
119. He S, Liang Y, Shao F, Wang X. Toll-like receptors activate programmed necrosis in macrophages through a receptor-interacting kinase-3–mediated pathway. *Proc Natl Acad Sci USA*. 2011;108:20054–20059.
120. Kaiser WJ, Sridharan H, Huang C, et al. Toll-like receptor 3-mediated necrosis via TRIF, RIP3 and MLKL. *J Biol Chem*. 2013;288:31268–31279.
121. Upton JW, Kaiser WJ, Mocarski ES. Virus inhibition of RIP3-dependent necrosis. *Cell Host Microbe*. 2010;7:302–313.
122. Guo H, Omoto S, Harris PA, et al. Herpes simplex virus suppresses necroptosis in human cells. *Cell Host Microbe*. 2015;17:243–251.
123. Kajava AV, Klopffleisch K, Chen S, Hofmann K. Evolutionary link between metazoan RHIM motif and prion-forming domain of fungal heterokaryon incompatibility factor HET-s/HET-s. *Sci Rep*. 2014;4:7436.
124. Davies KA, Tanzer MC, Griffin MD, et al. The brace helices of MLKL mediate interdomain communication and oligomerisation to regulate cell death by necroptosis. *Cell Death Differ*. 2018. https://doi.org/10.1038/s41418-018-0061-3.
125. Xie T, Peng W, Yan C, Wu J, Gong X, Shi Y. Structural insights into RIP3-mediated necroptotic signaling. *Cell Rep*. 2013;5:70–78.
126. Cook W, Moujalled D, Ralph T, et al. RIPK1-and RIPK3-induced cell death mode is determined by target availability. *Cell Death Differ*. 2014;21:1600.
127. Zhao J, Jitkaew S, Cai Z, et al. Mixed lineage kinase domain-like is a key receptor interacting protein 3 downstream component of TNF-induced necrosis. *Proc Natl Acad Sci USA*. 2012;109:5322–5327.

How to cite this article: Nanson JD, Kobe B, Ve T. Death, TIR, and RHIM: self-assembling domains involved in innate immunity and cell-death signaling. *J Leukoc Biol*. 2019;105:363–375. https://doi.org/10.1002/JLB.MR0318-123R